# TABLES FOR THE CHARACTERIZATION OF PLASTIC HINGES OF HOLLOW CIRCULAR RC COLUMNS FOR BRIDGES

JC. Pantoja[(1)], D. Chanchay[(2)], K. Velez[(3)],

*[(1)] Assistant Professor, Science and Engineering College, Universidad San Francisco de Quito, Quito, Ecuador, jcpantojam@usfq.edu.ec*
*[(2)] Research assistant, Science and Engineering College, Universidad San Francisco de Quito, Quito, Ecuador, dchanchay@estud.usfq.edu.ec*
*[(3)] Research assistant, Science and Engineering College, Universidad San Francisco de Quito, Quito, Ecuador, kvelezh@estud.usfq.edu.ec*

## *Abstract*

Hollow reinforced concrete columns are usually used in bridges for their structural benefits such as seismic mass reduction, lateral strength increase, and foundation design forces reduction. For the design of these elements, it is necessary to perform a non-linear analysis to estimate their behavior under gravitational and lateral loads besides determining the overall structural performance. Since the nonlinear analysis requires to model the plastic behavior of elements, the designer must characterize the flexural behavior of primary structural elements as columns. In this research, we study columns reinforced with a single layer of steel in the exterior face. Also, based on the literature available, it was selected the main variables to estimate the flexure behavior of these elements, and three limit states immediate occupation IO, life security LS and collapse prevention CP were proposed based on strain materials for distinguished flexure and compression behavior. A parametric analysis was performed for the variables of concrete strength of 35 MPa and 40 MPa, axial load ratio of 0.1 and 0.2, longitudinal steel ratio between 1% and 2%, transverse steel ratio by spirals of 1%, 1.5%, 2%, 2.5% and 3% and external thickness to diameter ratios of 0.1, 0.12 and 0.14. A total of 180 of hollow circular reinforced concrete columns were modeled by strip methodology accounting the materials stress-strain curves and confined stress on concrete. For the moment-curvature curve of each column, we determine the bilinear moment-curvature plastic hinge and the location of curvatures to reach the limit states. The results were organized in two types of charts: Type 1 normalize a bilinear moment-curvature curve and Type 2 characterize the limit states curvatures. Finally, the relative error was found to be less than 5% for deformation energy developed by the model proposed, and less than 1% in the moment-curvature obtained values compared with the analytical model.

*Keywords: Hollow columns; curvature; limit states; performance levels; plastic hinge.*

## 1. Introduction

Bridges are massive structures with multiple functionalities, mainly communication, but often they become important tourism points inside the city. Contrary to buildings, the overall structure concept design is to protect the strong-beam (superstructure) and to concentrate the plastic behavior on weak-column. Their superstructure is designed for gravitational loads mainly and often defined through the length of their spans. On the other hand, their substructure often is composed of monopiles or multiple piles framing with top cap beams where pile height is determined for topographic characteristics. Further, these piles must support lateral load effects as produced by seismic ground motion. For bridges structures with high levels of importance, this particular configuration requires nonlinear procedures that involve response time history analysis to determinate engineering demand parameters (EDP). Due to a non-linear analysis requires the estimation of the response beyond yield strain on materials and the degradation of the stiffness of the cross-section, the common practice to consider this effect is to concentrate the nonlinear flexure response through a bilinear rotational plastic hinge. The effort to obtain those parameters require to model cross-sectional geometric of beams and columns to calculate moment curvatures behavior; this step is needed to define the strain limits to guarantee the correct behavior of the section under several seismic hazard levels.

In past years, the hollow reinforced concrete (RC) column section has been studied mainly due to cost savings in construction and high bending strength resistance compared with a solid column with the same dimensions. Their lightweight for unit length reduces the seismic lateral force, design moments and simultaneously foundation size requirements; moreover, the cracking of the concrete produced for the chemical reaction due to the hydration of Portland cement is reduced due to the smaller volume of concrete as well as the minimum flexural reinforcement required by design code. All these characteristics result in higher strength–mass and stiffness–mass ratios, as well as higher bending and torsional stiffness. Since the structural response of the hollow column under seismic loading changes from a similar solid column, the assessment of their nonlinear behavior is required. Zahn, Park, & Priestley [1] studied hollow circular RC columns with on layer of longitudinal and spiral reinforcement placed near the outside face of section. They concluded that if the neutral axis is close to the unconfined inside face of the hollow section, ductile flexural behavior is expected; on the other hand, if the neutral axis is away from this inside face, early vertical splitting, crushing of concrete and low ductility arise. Further, they established that the factors to controls flexural ductility are the axial load ratio ($P/f'_cA_g$), the inside to outside diameter ratio (Di/D), the longitudinal steel ratio $r_l$, and materials strength $f_y$ and $f'_c$. Finally, they conclude that ductility can be achieved with low axial load, small longitudinal steel ratio, besides that the wall thickness should not be less than 15 percent of the overall section diameter and that longitudinal concrete strain at inside face to determine the ultimate curvature should be limited to 0.008.

Later Lee, Choi, Hwang, and Kwahk [2], conclude that hollow circular columns with a single layer of reinforcement can result in economical designs with limited ductility capacity which will often be adequate since ductility demand of tall piers is generally low, besides flexure-controlled section showed similar behavior to that of solid circular columns. Additionally, the displacement ductility factor increases proportionally to increase of transverse steel ratio near the outside face. Finally, for compression-controlled sections, the existence of the inside transverse steel could reduce the damaged area of the inside wall face, although a non-significant increase of ductility. Further, Liang and Sritharan [3] recommend that for thickness to outside diameter ratio (t/D) equal to 0.1, the element should be designed with a single layer of confinement reinforcement due to minimal increase in the ductility and reinforcement congestion in construction. Moreover, they limit the concrete strain at inside face to 0.005 or the strain at the outer edge of the core to confined crushing strain to obtain a satisfactory ductile behavior.

In this paper, a parametric analysis of hollow circular RC columns was developed based on the state of knowledge. The parameter axial load ratio $P/f'_cA_g$, the inside to outside diameter ratio Di/D, the thickness to outside diameter ratio t/D, the longitudinal and transversal steel ratio $\rho_l$ and $\rho_{tr}$ respectively, and materials strength $f_y$ and $f'_c$ were analyzed. Fig. 1 shows the dimension nomenclature of hollow columns. A total of 180 cross-sectional were modeled to obtain tables for the characterization of plastic hinges of hollow circular RC columns for bridges piles; also we developed tables to define the limit state of Immediate Occupancy (IO), Life Security (LS) and collapse prevention (CP) for each configuration. In each table, ductile and brittle failure in hollow columns was determined. The objective is applying these tables to the daily design of bridge projects.

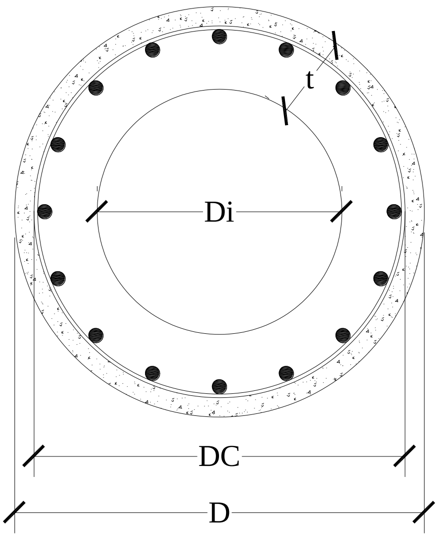


Fig. 1 – Schematic geometric of the hollow RC column.

## 2. Parametric Modeling

180 cross-sectional of hollow circular RC columns were modeled through the program Xtract [4] o develop the parametric analysis. The variables to consider and their range are listed next:

(1) The compressive strength of the concrete $f'_c$ will range from 30 to 40 MPa.

(2) The yield strength of reinforcement $f_y$ is set up to 420 MPa.

(3) The values of thickness to outside diameter ratio t/D used are 0.1, 0.12, and 0.14.

(4) The axial load ratio $P/f'_c A_g$ will be in the range of 0.1 and 0.2

(5) The longitudinal steel ratio ($\rho_l$) will be analyzed for 1%, 1.5%, and 2%.

(6) The transversal steel ratio ($\rho_{tr}$) will be analyzed for 1%, 1.5%, 2%, 2.5% and 3%. It is considered spiral transverse reinforcement for this analysis.

The parameters of analysis and their ranges were selected based on available literature for granted the more extensive practical application on bridge design.

## 3. Limit States

Based on the research of literature, three limit states for hollow circular RC columns were defined independently for compression controlled and tension-controlled failure: Immediate occupation (IO), life security (LS), and collapse prevention (CP). For the American Society of Civil Engineers [5], these limit states indicate correlations between the non-linearity of the materials where you can see the interaction of changes in structural stiffness and deformability according to a gradual creation of the ductile plastic label.

3.1 Immediate Occupancy Level:

In this state, there are fissures in the column cross-section, but there is any change of the flexural capacity. The element is working in the elastic range; as a result, it maintains the original stiffness and resistance. For both compression- and tension-controlled behavior, a limit in the unconfined concrete strain $\varepsilon_c = 0.003$ was select.

3.2 Life Security Level:

In this state, the longitudinal reinforcement is expected to be yield through the plastic length. The cross-section shows the beginning of inelastic behavior. We limit the cover strain of the cover concrete of 0.004 for compression-controlled sections and 0.005 for flexion-controlled sections.

3.3 Collapse prevention Level:

In this state, the strain of the material is limited to guarantee a ductile behavior under cyclic load. For compression failure, we control the first occurrence of two criteria: The inside strain of unconfined concrete reaches the value of 0.005, or the outside strain reaches the ultimate strain of $\varepsilon_{cu}$. In this state, the steel reinforcement remains with a strain before the ultimate reduce strain $\varepsilon_{suR}$. Finally, for tension-controlled sections, this limit is reached when the longitudinal steel reinforcement gets the ultimate strain $\varepsilon_{suR}$. The resume of strain limits of materials for each limit state level is shown in Table 1.

Table 1 – Strain limits of materials for limit states considerer

| **Failure controlled by** | **CP** | **LS** | **IO** |
|---|---|---|---|
| Compression | Inside face strain on concrete<br>$\varepsilon_c = 0.005$<br>or<br>$\varepsilon_c = \varepsilon_{cu}$ | Cover concrete strain<br>$\varepsilon_{cov} = 0.004$ | Cover concrete strain<br>$\varepsilon_c < 0.003$ |
| Flexure | Failure of longitudinal reinforcement<br>$\varepsilon_s = \varepsilon_{suR}$ | $\varepsilon_{cov} = 0.005$ | $\varepsilon_c < 0.003$ |

## 4. Analytical modeling procedure

Similar to models developed for Zahn [1], the cross-section of columns is analyzed by a strip discretization, where each strip is characterized by an area, stress vs strain curve of the material, and the coordinates of its centroidal area. The strain in materials is assumed that remains constant within the strip area; also, plane sections hypothesis is considered. The values of stresses and strain of materials are calculated at the centroid of the strip. After the modeling process, the flexural behavior of cross-section is obtained by moment-curvature analysis, besides the materials strain in cover concrete $\varepsilon_{cov}$, strain at inside face concrete $\varepsilon_c$, and strain of steel in tension $\varepsilon_s$. The process is defined in four steps, geometric definition, materials, axial load, and results. The main consider points are described next:

(1) The unconfined and confined concrete is modeled through Mander, Priestley & Park [6] stress-strain model. Eq. (1) to Eq. (3) describe the stress-strain equation used.

$$f_c = \frac{r f'_{cc}}{r-1+x^r} \tag{1}$$



 

Where,

$$r = \frac{E_c}{E_c - E_{sec}} \tag{2}$$

$$E_{sec} = \frac{f'_{cc}}{\varepsilon_{cc}} \tag{3}$$

(2) The maximum compressive strength of unconfined concrete ($f'_{co}$) for experimental models is set to $0.85f'_c$. The corresponding strain $\varepsilon_{co} = 0.002$, the crushing strain is $2\varepsilon_{co} = 0.004$, and its spalling strain is set to 0.005. The R factor is set to 3 as recommended Zahn [1] for hollow circular RC columns. The Eq. (1) is used to describe the stress vs strain curve of concrete setting $f'_{cc} = f'_{co}$ and $\varepsilon_{cc} = \varepsilon_{co}$.

$$f'_{cc} = f'_{co}\left(2.254\sqrt{1 + \frac{7.94 f'_l}{f'_{co}}} - \frac{f'_l}{f'_{co}} - 1.254\right) \tag{4}$$

Where,

$$\varepsilon_{cc} = \varepsilon_{co}\left[1 + R\left(\frac{f'_{cc}}{f'_{co}} - 1\right)\right] \tag{5}$$

$$f'_l = K_e \, \frac{1}{2} \, \rho_s \, f_{yh} \tag{6}$$

$$\rho_s = \frac{4 A_b D_c}{s\left({D_c}^2 - {D_i}^2\right)} \tag{7}$$

$$\varepsilon_{cu} = 0.004 + \frac{0.6\, \rho_s \, f_{yh} \, \varepsilon_{su}}{f'_{cc}} \tag{8}$$

(3) For the confined concrete, Eq. (4) to Eq. (8) were used, where $A_b$ is the area of spiral bar; $f_{yh}$ is the yield strength of spiral; Dc is the diameter of confined column measure between outside edges of the spiral, and $D_i$ is the inside diameter of the column. Hoshikuma & Priestley [7] recommended that to model hollow circular RC columns with a single layer of longitudinal and spiral reinforcement, the value of $K_e = 0.6$ produces a satisfactory result in a design application.

(4) The steel reinforcement is considered with a parabolic strain hardening steel model. The yield stress $f_y$ is set to 420 MPa, the fracture stress $f_u$ to 550 MPa, the strain hardening strain $\varepsilon_{sh}$ and the ultimate strain $\varepsilon_{su}$ is set up according to the bar area as recommended CALTRANS [8]; Table 2 and Table 3 specify the values used.

(5) The axial load in each column was applied uniformly through the cross-section based on the axial load ratio.

Table 2 – Ultimate Strain limits of steel $\varepsilon_{su}$

| $\varepsilon_{su}$ | **Specification [in$^2$]** |
|---|---|
| 0.120 | $A_s \leq 1.40$ |
| 0.090 | $A_s > 1.40$ |



 

Table 3 – Strain Hardening limits of steel $\varepsilon_{sh}$

| $\varepsilon_{sh}$ | Specification [in$^2$] |
|---|---|
| 0.0150 | $A_s \leq 0.85$ |
| 0.0125 | $0.85 < A_s \leq 1.15$ |
| 0.0115 | $1.15 < A_s \leq 1.80$ |
| 0.0075 | $1.80 < A_s \leq 3.00$ |
| 0.005 | $A_s > 3.00$ |

Zahn [1] constructed and tested six circular hollow RC column; for each one, they obtained experimental moment-curvature curves, also we model column unit 3, and we compared the results obtained. Table 4 describes the characteristics of the experimental unit 3 column, further in Fig. 2 is compared the results obtained from the experimental and analytic analysis, it can be concluded that the process of modeling coincides with the experimental results with errors ranging between 1% to 6 % for moment-curvature values.

Table 4 – Experimental characteristics of column unit 3, Zahn [1]

| Description | Value | Units |
|---|---|---|
| $f'_c$ | 29.6 | MPa |
| Outside diameter D | 400 | mm |
| Inside diameter $D_i$ | 250 | mm |
| Axial load ratio | 10 | % |
| Axial load | 224.96 | kN |
| $\rho$ longitudinal | 4.2 | % |
| $\rho$ Transverse | 2.18 | % |
| Spiral spacing S | 7.5 | mm |
| Reinforcement | 16 Ø 16 | mm |
| Spiral bar diameter | 12 | mm |



 

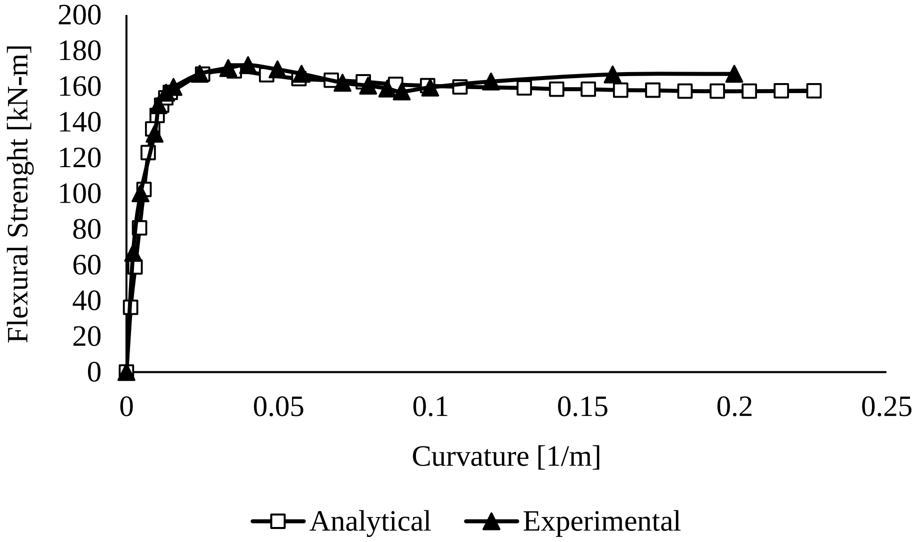


Fig. 2 – Experimental moment-curvature curve of Column Unit 3, Zahn [1], and comparison with analytical results obtained with Xtract [4].

## 5. Normalized Design chart for characterizing plastic hinge

Based on the results of the parametric analysis of the hollow circular RC column describe previously, two types of normalized design charts were derived. The variables to use in these charts are the axial load ratio $P/f'_cA_g$, the thickness to outside diameter ratio t/D, the longitudinal and transversal steel ratio $\rho_l$ and $\rho_{tr}$ respectively, and concrete $f'_c$. The chart Type 1 characterizes a bilinear moment-curvature hinge with residual resistance defining the points A to E as defined in AISCE 41-13 [5]; The chart Type 2 normalizes the curvature required to reach the limit states IO, LS and CP based in yield curvature $\phi_y$. The Fig. 3 describes the schematic configuration of the moment-curvature plastic hinge and the location of limits states.

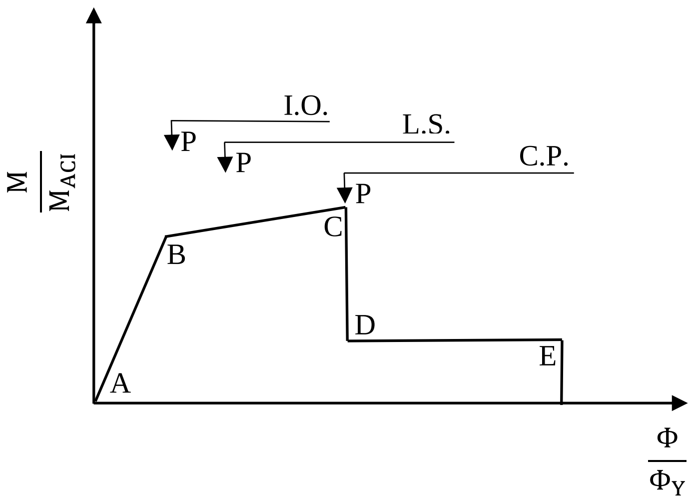


Fig. 3 – Schematic configuration of normalized moment-curvature hinge and location of limit states.



 

In this study, only the location of service levels for primary structures is considered, since columns are being analyzed. The segment $\overline{AB}$ corresponds to the elastic behavior of the element, where point B corresponds to the flexural yield of the section. The segment $\overline{BC}$ corresponds to the deformations that occur after yield, therefore, characterize the plastic behavior of the element. The segment $\overline{DE}$ is considered in this analysis as 10% of flexural strength at point C and corresponds to $2\varepsilon_{cu}$. For bending, the curves will be normalized as the flexural strength of the hollow circular RC concrete column to the nominal uniaxial flexural strength $\frac{M}{M_{ACI}}$ for a solid circular column equivalent with outside diameter D and axial load P. This value is estimated by a P-M interaction diagram based in ACI-318 [9]. For curvature, the normalization will be a function of the section curvature of the hollow section to yield curvature ratio $\frac{\emptyset}{\emptyset_y}$, where $\emptyset = \frac{M_y}{E_c \times I_{efective}}$.

After the design process for gravity loads, cross-sectional dimensions of columns, as well as the longitudinal and transversal reinforcement, are defined. The first step is to calculate the values of $f'_c$, $P/f'_cA_g$, t/D, $\rho_l$, $\rho_{tr}$ for the column to use the charts. Next, compute the flexural strength $M_{ACI}$ and the yield curvature $\emptyset_y$. After that, with the values obtained in step 1, select the corresponding chart Type 1 and Type 2. With $M_{ACI}$ and $\phi_y$ calculated, determine the values of moment and curvature for points A to E of the bilinear plastic hinge as well as the values of curvature for IO, LS, and CP limit states. Table 5 and Table 6 shows an example of Type 1 and Type 2 design chart, respectively.

Table 5 – Type 1 Chart: Normalized bilinear moment-curvature hinge

| $f'_c$ = 30 MPa | | | | | |
|---|---|---|---|---|---|
| t/D =0.12 | | | | | |
| $\frac{P}{f'c\,Ag}$ | $\rho_{tr}$ [%] | $\rho_l$ [%] | $\frac{\phi_{IO}}{\phi_{fy}}$ | $\frac{\phi_{LS}}{\phi_{fy}}$ | $\frac{\phi_{CP}}{\phi_{fy}}$ |
| 0.1 | 1.00 | 1 | 4.7 | 5.7 | 22.3 |
| | | 1.5 | 3.9 | 4.7 | 14.2 |
| | | 2 | 3.8 | 4.9 | 11.6 |
| | 1.50 | 1 | 4.4 | 5.8 | 28.1 |
| | | 1.5 | 3.7 | 4.8 | 16.6 |
| | | 2 | 3.4 | 4.3 | 12.5 |
| | 2.00 | 1 | 4.9 | 8.2 | 35.1 |
| | | 1.5 | 4.2 | 5.6 | 19.1 |
| | | 2 | 3.8 | 4.9 | 14.0 |
| | 2.50 | 1 | 4.9 | 8.2 | 34.9 |
| | | 1.5 | 4.6 | 6.1 | 20.0 |
| | | 2 | 4.1 | 5.4 | 14.5 |
| | 3.00 | 1 | 4.9 | 8.2 | 34.7 |
| | | 1.5 | 4.7 | 7.9 | 33.5 |
| | | 2 | 3.0 | 4.4 | 14.8 |



 

Table 6 – Type 2 Chart: Normalized curvature limit states IO, LS and CP.

| f´c = 30 MPa; $\frac{P}{f'c\,Ag}$ = 0.1 ; t/D=0.12 | | | | | | | |
|---|---|---|---|---|---|---|---|
| | | $\rho_l$ = 1% | | $\rho_l$ = 1.5% | | $\rho_l$ = 2 % | |
| P transverse [%] | Punto | $M/M_{ACI}$ | $Ø/Ø_Y$ | $M/M_{ACI}$ | Ø/ØY | $M/M_{ACI}$ | $Ø/Ø_Y$ |
| 1.000 | 0.000 | 0.000 | 0.000 | 0.000 | 0.000 | 0.000 | 0.000 |
| | A | 0.474 | 1.000 | 0.482 | 1.000 | 0.481 | 1.000 |
| | B | 0.522 | 22.255 | 0.528 | 17.336 | 0.542 | 23.890 |
| | C | 0.047 | 22.255 | 0.048 | 17.336 | 0.048 | 23.890 |
| | D | 0.047 | 44.510 | 0.048 | 34.671 | 0.048 | 47.780 |
| | E | 0.000 | 44.510 | 0.000 | 34.671 | 0.000 | 47.780 |
| | | | | | | | |
| 1.500 | A | 0.480 | 1.000 | 0.487 | 1.000 | 0.477 | 1.000 |
| | B | 0.540 | 29.450 | 0.550 | 23.005 | 0.537 | 19.781 |
| | C | 0.048 | 29.450 | 0.049 | 23.005 | 0.048 | 19.781 |
| | D | 0.048 | 58.900 | 0.049 | 46.009 | 0.048 | 39.562 |
| | E | 0.000 | 58.900 | 0.000 | 46.009 | 0.000 | 39.562 |
| | | | | | | | |
| 2.000 | A | 0.489 | 1.000 | 0.494 | 1.000 | 0.483 | 1.000 |
| | B | 0.552 | 35.059 | 0.569 | 28.571 | 0.555 | 24.289 |
| | C | 0.049 | 35.059 | 0.049 | 28.571 | 0.048 | 24.289 |
| | D | 0.049 | 70.118 | 0.049 | 57.143 | 0.048 | 48.578 |
| | E | 0.000 | 70.118 | 0.000 | 57.143 | 0.000 | 48.578 |
| | | | | | | | |
| 2.500 | A | 0.489 | 1.000 | 0.501 | 1.000 | 0.487 | 1.000 |
| | B | 0.555 | 34.859 | 0.578 | 32.361 | 0.567 | 27.430 |
| | C | 0.049 | 34.859 | 0.050 | 32.361 | 0.049 | 27.430 |
| | D | 0.049 | 69.718 | 0.050 | 64.722 | 0.049 | 54.860 |
| | E | 0.000 | 69.718 | 0.000 | 64.722 | 0.000 | 54.860 |
| | | | | | | | |
| 3.000 | A | 0.489 | 1.000 | 0.504 | 1.000 | 0.495 | 1.000 |
| | B | 0.559 | 34.695 | 0.585 | 33.548 | 0.578 | 31.087 |
| | C | 0.049 | 34.695 | 0.050 | 33.548 | 0.050 | 31.087 |
| | D | 0.049 | 69.390 | 0.050 | 67.095 | 0.050 | 62.175 |
| | E | 0.000 | 69.390 | 0.000 | 67.095 | 0.000 | 62.175 |

## 5. Normalized Charts Validation

For the process of validation, a column was model in the software XTRACT [4]. We obtained the analytical moment-curvature and determined the curvatures at IO, LS, and CP service levels. Next, we calculate the bilinear moment-curvature behavior of the column with charts Type 1 and determine the curvature service levels with chart Type 2. Table 7 shows the validation column characteristic, and Fig. 4 compares the obtained results. It can be concluded that there is consistency in the deformation energy developed, with relative error in values near to 1%.

Table 7 – Geometric characteristic of validation column

| **Parameter** | **Value** |
|---|---|
| Outside Diameter D [m] | 1.50 |
| Inside Diameter Di [m] | 1.14 |
| t/D | 0.12 |
| $f'_c$ [MPa] | 35 |
| $f_y$ [MPa] | 420 |
| $\rho$ Transverse [%] | 1.5 |
| $\rho$ Longitudinal [%] | 1.0 |
| $\frac{P}{f'_c A_g}$ | 0.1 |

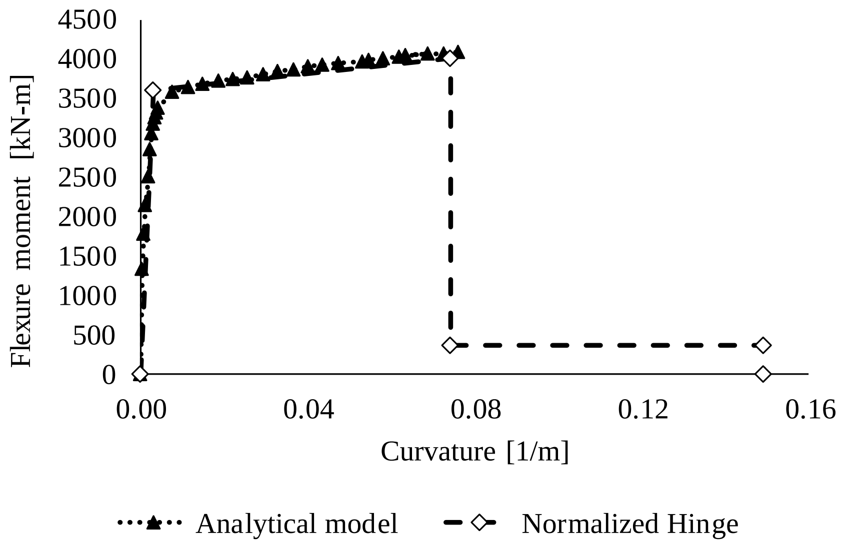


Fig. 4 – Comparison between the moment-curvature curve obtained with analytical modeling and by normalized charts.

## 6. Conclusions and Recommendation

Hollow reinforced concrete columns are used for their low mass and higher bending and torsional stiffness than a similar solid RC column. For this evaluation, computer models of 180 hollow circular RC columns were utilized. We investigate the nonlinear behavior of hollow circular columns analyzing their moment-curvature curve; also, we define the curvature to reach three limit states IO, LS, CP. The charts developed are available on request from the corresponding author. The key conclusions of this study are presented next:

(1) In general, a ductile behavior in hollow circular columns is reached for low axial load and longitudinal steel reinforcement ratio; besides, the thickness to outside diameter ratio (t/D) ranging from 0.1 to 0.14.

(2) For axial load ratios $\frac{P}{f'c\,Ag} = 0.2$, the failure mode of the column is fragile, and confined concrete reaches the crushing strain $\varepsilon_u$ at the inside face for all cross-section modeled. For this reason, a ductile behavior is obtained to axial load ratios less than 0.1.

(3) Transverse steel ratios between 2 – 3% results in ductile behavior only if $\rho_l$ is less than 1%.

(4) The charts successfully represent the non-linear behavior of the cross-section with a relative error of less than 5% in the deformation energy developed, and less than 1% in the moment-curvature obtained values compared with the analytical model.

(5) It is necessary to extend this study to consider the interaction of shear stress since it can significantly change the nonlinear behavior of columns.

(6) Finally, further research is required to estimate the plastic hinge length in this type of cross-section, since the current practice to estimate this value is by the model proposed by Priestley and Park [10] based mainly in solid columns.

## 7. Acknowledgments

We wish to thank Universidad San Francisco de Quito for supporting this study and for the financial support for attending the conference. Special thanks are extended to Katherine Velez and Diego Chanchay for their work daily as assistance research in this study.

## 6. References

[1] Zahn, F. A., Park, R., & Priestley, M. J. N. (1990). Flexural strength and ductility of circular hollow reinforced concrete columns without confinement on the inside face. Structural Journal, 87(2), 156-166.

[2] Lee, J. H., Choi, J. H., Hwang, D. K., & Kwahk, I. J. (2015). Seismic performance of circular hollow RC bridge columns. KSCE Journal of Civil Engineering, 19(5), 1456-1467.

[3] Liang, X., & Sritharan, S. (2018). Effects of confinement in circular hollow concrete columns. Journal of Structural Engineering, 144(9), 04018159.

[4] Chadwell, C. (2007). XTRACT (Nº de version 3.0.8). Windows. Rancho Cordova: TRC Bridge Design Software.

[5] Pekelnicky, R., Engineers, S. D., Chris Poland, S. E., & Engineers, N. D. (2012). ASCE 41-13: Seismic evaluation and retrofit rehabilitation of existing buildings. Proceedings of the SEAOC.

[6] Mander, J. B., Priestley, M. J., & Park, R. (1988). Theoretical stress-strain model for confined concrete. Journal of structural engineering, 114(8), 1804-1826.

[7] Hoshikuma, J. I., & Priestley, M. J. N. (2000). Flexural behavior of circular hollow columns with a single layer of reinforcement under seismic loading. SSRP, 13.

[8] Caltrans, S. D. C. (2010). Caltrans seismic design criteria version 1.6. California Department of Transportation, Sacramento.

[9] ACI Committee 318. (2019). Building Code Requirements for Structural Concrete (ACI 318-19): An ACI Standard: Commentary on Building Code Requirements for Structural Concrete (ACI 318R-19). American Concrete Institute.

[10] Priestley, M. J. N., & Park, R. (1987). Strength and ductility of concrete bridge columns under seismic loading. Structural Journal, 84(1), 61-76.



 